Journal of Applied Polymer Science

Synthesis of clay–TiO_2 nanocomposite thin films with barrier and photocatalytic properties for food packaging application

Hojatollah Bodaghi,[1] Younes Mostofi,[2] Abdulrasoul Oromiehie,[3] Babak Ghanbarzadeh,[4] Ziba Ghasimi Hagh[1]

[1]Department of Horticulture Science and Plant Protection, College of Agriculture, University of Shahrood, Shahrood, Iran
[2]Department of Horticulture Science, College of Agriculture & Natural Resources, University of Tehran, Karaj, Iran
[3]Iran Polymers and Petrochemical Institute, Tehran 1499713115, Iran
[4]Department of Food Science and Technology, Faculty of Agriculture, University of Tabriz, Tabriz, Iran
Correspondence to: H. Bodaghi (E-mail: hbodaghi@shahroodut.ac.ir)

ABSTRACT: In this study, low-density polyethylene (LDPE) nanocomposite films with two types of nanoparticles, TiO_2 (3 wt %) and Closite 20A (3 and 5 wt %), were prepared using a melt blow extrusion as an industrial method and their properties such as mechanical properties, water vapor, oxygen and carbon dioxide gas barrier, and antimicrobial activity were tested. Transmission electron microscopy (TEM) and X-ray diffraction (XRD) were also performed to determine the degree of dispersion and exfoliation of nanoparticles. Mechanical test indicated that the reinforcement in the presence of the nanocomposites was more than that with their conventional counterparts, and the highest stiffness was achieved in a sample containing 5 wt % clay and 3 wt % TiO_2. Exfoliation of silicate layers and a good dispersion of TiO_2 nanoparticles in LDPE were achieved as confirmed by XRD and TEM. The gas barrier properties were improved after formation of the nanocomposites especially by insertion of 5 wt % of clay nanoparticles as a filler in the LDPE matrix. The photocatalytic effect of the nanocomposite film was carried out by antimicrobial evaluation against *Pseudomonas* spp. and *Rhodotorula mucilaginosa* and by ethylene removal test using 8 W ultraviolet (UV) lamps with a constant relative intensity of 1 mW cm^{-2}. The greatest effects were recorded by combining UVA illumination and active film. It was also proven that the photocatalyst thin film with improved barrier properties prepared by extrusion could be used in horticultural product packaging applications. © 2014 Wiley Periodicals, Inc. J. Appl. Polym. Sci. **2015**, *132*, 41764.

KEYWORDS: clay; films; packaging; X-ray

Received 4 July 2014; accepted 1 November 2014
DOI: 10.1002/app.41764

INTRODUCTION

Petroleum–plastic materials such as polyethylene (PE), polypropylene (PP), and polystyrene (PS) dominate current plastics market because of their high strength, light weight, low cost, and good barrier properties.[1] Annually, more than 40% of the plastics are used for packaging with almost half them are used for food packaging in the form of films, sheets, bottles, cups, tubes, and trays.[2] The simplest and the most inexpensive plastics made by addition polymerization of ethylene is PE. Low-density polyethylene (LDPE) is the most commonly used packaging film owing to its excellent process ability, chemical inertness, safety in using for contact with food materials, good heat sealing property, and low production cost.[3] Some limitation in physicochemical properties of such plastic packaging materials restricts their application in the packaging industry. Most of the polyolefin-based packaging materials have a good water vapor barrier properties, while their barrier properties against oxygen and carbon dioxide are poor with low stiffness and tensile strength.[4] These limitations in plastic material properties should be improved to extend their usage in food packaging application.

The inorganic mineral fillers help in improving polymer performance properties, such as increasing the stiffness, heat distortion temperature, barrier properties, hardness, and toughening of the products.[5–7] The properties of polymer composition can be affected by the particle size, shape loading, interfacial bonding, and dispersion of the additives.[8] Inorganic nanomaterials such as titanium dioxide (TiO_2),[9–12] silicon dioxide (SiO_2),[13–16] and different types of organoclays[1,17–20] have been used to fulfilling polymer properties. Recently, nanocomposites have been proven to be a promising option in order to improve barrier and mechanical properties of base polymer. A polymer matrix reinforced with nanoparticles having at least one dimension in the nanometer range [e.g., silicate-layered clay-like montmorillonite (MMT)] exhibits much improved properties owing to

high aspect ratio and high surface area of nanoparticles.[1] The reinforced nanocomposites exhibited mechanical, thermal, and barrier properties.

Application of photocatalytic semiconductor oxides emerges as a successful technology to struggle against biological risks. Among these functional materials, organic and inorganic nanoparticles have had noticeable increasing attraction owing to their unique properties.[21,22] One of the most effective of photocatalyst is TiO_2 owing to its strong properties, safety, and long-term physicochemical stability.[23] It has been widely used as a self-cleaning and self-disinfecting material for surface coating in many application.[24,25] The photocatalytic effect of TiO_2 has been used to inactive a wide spectrum of microorganisms.[23,26–28] When TiO_2 particles were irradiated with ultraviolet (UV) light with wavelength of <385 nm, the photogenerated holes and electrons react with water and oxygen, respectively, to form hydroxyl radicals (•OH) and reactive oxygen species (O_2^-), these strong oxidizing agents can decompose organic and inorganic contamination on the surface of TiO_2.[23,27]

Recently, the removal of ethylene gas by TiO_2 photocatalysis has received wide interest from a number of researchers.[13,23,27,29–31] Ethylene is a plant hormone that possibly causes deterioration of fresh market crop products and is a primary contaminant in package and storage atmospheres.[32] The removed ethylene and/or inhibition effects of ethylene in the stored environment is fundamental to maintaining postharvest quality of horticultural crops.

In the late 1980s, the report from the Toyota research group of a nylon-6 (N6)/montmorillonite (MMT) nanocomposite, for which very small amounts of layered silicate loadings resulted in pronounced improvements of thermal and mechanical properties.[33] Thereafter, numerous studies were done on the polymer/clay nanocomposites in various industrial applications including in packaging industry.[1,34] Improved barrier properties in packaging prolong the food shelf life via restricting humidity or substances such as oxygen, ethylene, aroma, or unusual flavors interacting with the food.[35] Clays in nanoscale offer several advantages over conventional microsized clays in polymer matrix, and improve thermal stability, mechanical and gas barrier properties without any significant reduction in other relevant properties.[36]

To the best of our knowledge, no work has been reported on the antimicrobial activity and barrier properties of polyolefin-based plastic/TiO_2–clay nanocomposite films for application in food packaging. So this work is devoted to preparation of melt-blown LDPE/clay–TiO_2 nanocomposite film and characterization of properties including physical, mechanical, morphological, and barrier properties with possible permeability restriction and antimicrobial activity of the nanocomposite films.

MATERIALS AND METHODS

Titanium oxide (TiO_2) nanoparticles in the Anatase and Rutile phase having range of 20–80 nm were purchased from Nanoshel. Closite 20A nanoparticles were provided by Sothern Clay Product, TX. Montmorillonite is suitable for incorporation in a nonpolar polymeric matrix such as PP and PE. LDPE LF200 (MFT 2 g min^{-1}) was purchased from Arak Petrochemical, Iran, and PE-MA Karaband LEH (1.7 mol MA groups) was purchased from Garankin, Iran. Glycerol (extra pure grade) was purchased from Mojallali, Iran. *Psudomonas* spp. and *Rhodotroula mucilaginosa* were used to test the antimicrobial activity of resultant films. These microorganisms were cultured in plate count broth and sabouraud dextrose broth (Oxide, Milan, Italy), respectively, using the appropriate times and temperature of incubation.

Preparation of Clay–TiO_2 Nanocomposite

Clay, TiO_2, and clay–TiO_2 nanocomposite films were prepared by the melt blending method. Modified TiO_2 (M-TiO_2) powder was obtained by mixing modified Anatase and Rutile phases in a weight ratio of 7 : 3. TiO_2 (total of 3 wt %), Closite 20A (3 and 5 wt %), PE-MA (3 wt %), glycerol (0.5 wt %), and LDPE granules were blended for 1 h using a mixer. M-TiO_2 was used to prevent agglomeration of the nanoparticles and to provide a uniform distribution of TiO_2 into the LDPE matrix. The mixture was extruded by a Brabender twin-screw compounder (model DSE 20, Germany) for incorporating nanoparticles into the LDPE matrix. For LDPE and its nanocompounds, a constant temperature of 130°C was used in all the zones of the extruder and the speed of the central screw was set to 120 rpm. The extrudate was cooled down in air at 23°C ± 3°C and pelletized. LDPE and nanocomposite films with a thickness of 30 ± 3 μm were finally obtained by a film-blowing machine. The resulting film containing TiO_2 nanoparticles had a milky whitish appearance.

Analysis and Characterization Techniques

Tensile tests, Young's modulus, stress and strain at break of the nanocomposites were obtained from on dumbbell samples in an Insron 6025 testing machine according to ISO standard 2–527 at a crosshead speed of 50 mm min^{-1}. An extensometer was used to determine the elongation within a gauge length of 50 mm.

X-ray Diffraction Pattern

Structure of pristine clay, TiO_2, and clay–TiO_2 nanocomposite films was evaluated with XRD patterns by using a Zimens D5000 diffractometer operated at 30 kV and 30 mA, equipped with Cu Kα radiation. The scanning range was from 2° to 40°.

Crystallization Behavior of Nanocomposites

Crystallization properties were studied by using a Netzesh (model 200F 3 Maia) differential scanning calorimeter (DSC). Samples were heated from 20 to 200°C at a rate of 10°C min^{-1} under a nitrogen atmosphere and held for 10 min to remove the thermal history before cooling at desired rate of 10°C min^{-1} and reheated to 200°C. Melting temperature (T_m, °C), melting enthalpy (ΔH_m in J g^{-1}), and crystallization temperature (T_c, °C) were obtained from the first heating and cooling run. Degree of crystallinity (X_c, %) was calculated using melting enthalpy of samples (for the composite samples after normalization for the polymer amount) according to the following equation:

Table I. Composition of Samples and Their Codes

Sample code	LDPE (wt %)	Compatibilizer (wt %)	Glycerol (wt %)	Closite 20A (wt %)	TiO_2 (wt %)
PE1	96.5	3	0.5	-	-
PE2	93.5	3	0.5	3	-
PE3	91.5	3	0.5	5	-
PE4	93.5	3	0.5	-	3
PE5	90.5	3	0.5	3	3
PE6	88.5	3	0.5	5	3

$$X_c, \% = \frac{\Delta H_m}{\Delta H_m^\circ} \times 100,$$

where ΔH_m° is the melting enthalpy of 100% crystalline form of PE.[37]

Transmission Electron Microscopy

Transmission electron microscopy (TEM) micrographs were obtained at 100 kV with a PHILIPS EM-2085 TEM controlled by a microprocessor.

Film Permeability Rates

The water vapor permeability rate (WVPR) was measured with a WVP tester, model L80–500 equipped with a very sensitive and reliable humidity sensor, which is located directly in the measuring chamber to control temperature and relative humidity. Oxygen (OPR) and carbon dioxide permeability rates (CDPR) through PE films (with and without nanoparticles) were obtained using an OX-TRAN 2/21 and PERMATRAN-C 4/41 (MOCON, Minneapolis, MN) at 25°C and 1 atm, respectively. The detection limit of the instrument was 0.05 cc-mil m^{-2} day^{-1}.

Antimicrobial Activity Evaluation

The antimicrobial activity against *Pseudomonas* spp. and *R. mucilaginosa*, representing the main microorganisms on fruit and vegetable crops.[38,39] The antimicrobial activity of PE6 film was assessed as described by Chawengkijwanich and Hayata[40] with some modifications. Each test film (6-cm diameter) was placed in sterilized Petri dishes under aseptic conditions. One milliliter of each microorganism stock solution (containing approximately 10^8 and 10^7 CFU mL^{-1} for *Pseudomonas* spp. and *R. mucilaginosa*, respectively) was pipetted onto each test piece in its Petri dish and a piece of transparent PE thin film was placed on the surface of the inoculated test film. In this way, the drop was completely spread over the test film surface. The Petri dish was covered tightly with polyvinyl chloride (PVC) film (5 μm thickness). Test samples were placed at a distance of 25 cm from six 8-WUVA black light bulbs (Actinic BL, Philips, Poland). The ultraviolet A light (UVA, wavelength 315–400 nm) intensity on the surface of the film test piece, as measured by a UVA-400 radiometer (S-365 UV-sensor, Iuchi, Osaka, Japan), was 1 mW cm^{-2}. As controls, film samples were stored under the same conditions without UVA light illumination (TiO_2–clay–nanocomposite film with no UVA), whereas other samples were stored under the same conditions without films, but receiving UVA light illumination (control). Samples were taken in three replicates at 60-min intervals for 3 h. Then, the sample test piece was removed from the light, 9 mL of sterile saline solution was added to the Petri dishes containing the test and PE films, and shaken for 180 s on a universal small shaker (IKA MS 3 digital, Germany). One milliliter of solution was withdrawn at each sampling event and diluted to 1/10, 1/100, 1/1000, and 1/10,000 with sterile saline solution. A volume of 0.1 mL of the undiluted and diluted solutions was plated over appropriate media. Three replicate plates were used for each solution. The media were from Oxoid (Milan, Italy). *Pseudomonas* agar base was incubated at 25°C for 48 h for *Pseudomonas* spp. and Sabouraud dextrose agar was incubated at 25°C for 48 h for *R. mucilaginosa* and the colony-forming units (CFUs) were counted.

Ethylene Removal Test

To evaluate the catalytic activity of nanocomposite film toward ethylene degradation, photocatalysis experiments were carried out by placing PE1 and PE6 film samples (sample area of ~200 cm^2) in a sealed 2.5-L gas-tight sampling bag consisting of a gas sampling port (GL Science, Tokyo). Ethylene was injected into the sampling bag to give a concentration of 10 ppm. The sampling bags were held at 25°C with ambient relative humidity (about 70–80%) under light illumination of six 8-WUVA black light bulbs (Actinic BL, Philips, Poland). The bulbs were located 20 cm above the film samples. The UVA light intensity reached the surface of sample films was approximately 1 mW cm^{-2}. Ethylene concentration in the sampling bags was measured periodically over 3 h using gas chromatography. Triplicate samples of each product were tested.

RESULTS AND DISCUSSION

Nanocomposites Mechanical Properties

Developed nanocomposite films including clay, TiO_2, and clay/TiO_2–LDPE nanocomposite films are noted in Table I. The results of determination of mechanical properties of the set of samples are collected in Table II. The results shown that the Young's modulus of the LDPE nanocomposites (PE2–PE6) was 1.1 to 1.6 times higher than for the PE1 (PE control) (Table II). It is observed that with application of Closite 20A as a clay nanoparticle, stiffer materials were therefore obtained (higher value in Young's modulus test), confirming the reinforcing effect of the nanoparticle in the polymer matrix, which is consistent with previously reported results.[19,35] It can also be concluded that the Young's modulus showed good enhancement with the

Table II. Mechanical Properties of the Different LDPE Composites

Sample	Young's modulus (MPa)	Stress at break (MPa)	Strain at break (%)
PE1	97.11 ± 4.6	11.62 ± 0.32	126.4 ± 19.3
PE2	126.6 ± 14.2	12.47 ± 0.26	117.8 ± 18.2
PE3	143.6 ± 15.4	12.63 ± 0.44	113.5 ± 17.5
PE4	107.7 ± 11.1	12.12 ± 0.47	131.6 ± 23.6
PE5	148.7 ± 17.2	12.24 ± 0.37	123.1 ± 22.4
PE6	153.4 ± 22.3	11.97 ± 0.34	118.1 ± 18.1

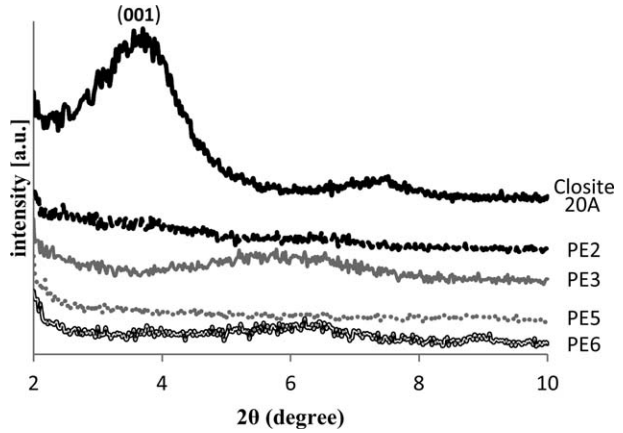

Figure 1. XRD spectrum of the result film with different clay content.

addition of TiO_2 nanoparticles as a filler so that, the highest Young's modulus value was observed in PE6 nanocomposite film and this enhancement is further seen with respect to interaction between both of nanoparticles, which is believed to be due to good interface between polymer and TiO_2, as also reported previously.[8] Tensile strength for LDPE/nanoclay, LDPE nano-TiO_2 composite, and combination of them increased at the blend composition of clay 3% and 5% with TiO_2 3% compared to control. This is because of good dispersion of nanofillers in the LDPE matrix that lead to the higher tensile strength. According to Liang *et al.*,[41] the dispersed nanoclay with high aspect ratio possesses a higher stress bearing capability and efficiency. Stronger interaction between nanoclay layers and polymer molecular associated with larger contact surface results in more effective constrain of the motion of polymer. Relative increase of strength stress in clay–TiO_2 nanocomposite may be due to difficult achievement of homogenous structure of nanoclay and nano-TiO_2 with LDPE. According to Golebiewski *et al.*,[17] at high filler loading, the nanoparticles is found in the form of microscale layer due to preferred stacking of the individual silicate layer in ordered structure (tactoids).

The strain at break versus blend composition of LDPE/nanoclay composite showed a decreasing pattern for all blend composition (Table I). Reduced strain at break may be due to low rate of compatibilizer, so that according to Golebiewski *et al.*,[17] the highest strain at break was achieved with application of 15% PE-MA as a compatibilizer in nanoclay–LDPE composites.

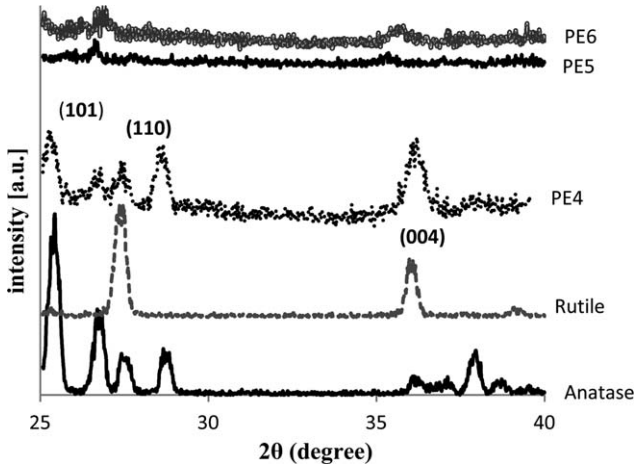

Figure 2. XRD spectrum of the result film with different TiO_2 content.

Table III. Thermal Properties of the Samples

Sample code	ΔH_m (J g^{-1})	T_c (°C)	$-\Delta H_m$ (J g^{-1})	T_m (°C)	X_c (%)
PE1	97.71	96.7	102.5	110.8	34.9
PE2	98.07	97.7	98.39	111.3	33.5
PE3	94.47	96.3	95.16	112.2	32.4
PE4	95.95	96.5	96.44	112.7	32.9
PE5	96.14	97.2	94.63	111.6	32.3
PE6	91.79	97.1	96.93	111.7	33.1

XRD Patterns

X-ray diffraction (XRD) measurement results of nanoparticles and its LDPE nanocomposite films are shown in Figures 1 and 2. Two diffraction peaks are observed for the org-clay (Closite 20 A) corresponding to basal spacing $d_{001} = 24.17$ Å ($2\theta = 3.88$) and $d_{002} = 11.90$ Å ($2\theta = 7.32$) (Figure 1). In the clay–TiO_2 nanocomposites, d_{001} and d_{002} peaks disappeared clearly. The general conclusion at this point is that compounding protocol for insertion of two nanoparticles in LDPE matrix may achieved significant improvement in the highest exfoliation of MMT with a smooth XRD curves. The appearance of the amorphous structure can be caused by complete exfoliation due to polymer–nanoclay compatibility. The results are comparable to Golebiewski *et al.*[17]

The XRD patterns of two nano-TiO_2 particles (Anatase and Rutile) and its nanocomposites are shown in Figure 2. A typical peak of Anatase at $2\theta = 25°$ was observed, corresponding to the diffraction of (101) and two typical peaks of Rutile at $2\theta = 27°$ and $2\theta = 36°$ corresponding to the diffractions of (110) and (004), showing that Anatase and Rutile were pure. These findings of the current test are consistent with those of Thamaphat *et al.*[42] The XRD curve of TiO_2–LDPE nanocomposites possesses the basal peaks of Anatase and Rutile indicating that all resultant films exhibit a pure Anatase and Rutile phase structures. Therefore, the polymerization process does not change the original crystal structure but nanoclay loading in the polymer matrix decreased the intensities of peak corresponding to TiO_2 nanopowder. A similar decrease in peak intensities of polymer and increase in peak intensity of TiO_2 was observed and reported by Mina *et al.*[43] while studying the XRD profile of PP/titanium dioxide composite. All these data suggested that nanoclay layers were exfoliated and TiO_2 particles were dispersed in the polymer matrix.

Thermal Analysis (DSC)

The melting temperature and the degree of crystallinity for the blown films were determined based on DSC measurements. The data are in Table III. As it is seen from the table, addition of different nanoparticles does not influence markedly the film melting temperature and the PE crystallinity in nanocomposite films. The results suggested that the addition of nanoparticles to neat LDPE did not change the degree of crystallinity. This implies that the nanoadditives does not act as a nucleating agent for LDPE matrix. Similar results were obtained in

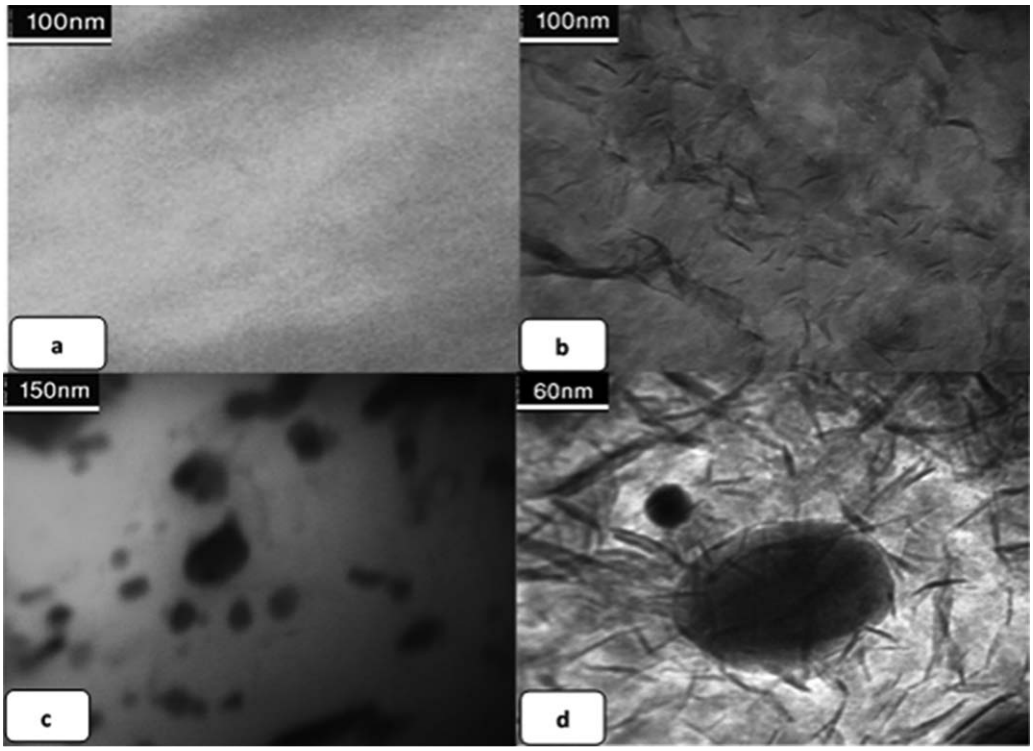

Figure 3. Scanning electron micrographs of nanocomposites: (a) PE1, (b) PE3, (c) PE4, and (d) PE6 films.

previous studies.[44,45] However, some studies also showed that nanoclay particles act as effective nucleating agent.[17,19] Consequently, further investigations are needed to clarify the effect of the size, chemical composition, compatibilizer content, and other agents in the nucleation activity and crystallization kinetics of polymers.

TEM

Dispersal of nanoparticles is somewhat critical. The presence of agglomerations of additives in the polymeric matrix is thought to cause breakage of the film and reduction in its qualities or plasticity.[46] TEM micrographs of PE control, exfoliated clay/LDPE nanocomposite, TiO_2/LDPE nanocomposite, and clay–TiO_2/LDPE nanocomposites are shown in Figure 3. The clear or white zones represent the polymeric matrix [Figure 3(a)], whereas the dark areas represent the nanoparticles. The distribution of the nanoclay in the film and good exfoliation of nanoparticles in the PE3 film are evident in Figure 3(b) and can confirm the result related to XRD analysis. Relative good dispersion of Anatase and Rutile in the PE4 is shown in Figure 3(c) and exfoliated clay nanoparticle with two nanoparticles of TiO_2 in the PE6 is shown in Figure 3(d). As reported by Kawasuni,[33] owing to nonpolar groups in the polyolefin backbone, the silicate layers of clay, even modified by nonpolar long alkyl groups, are polar and incompatible with polyolefin. This makes the study of the different parameters and variable involved in the development of a nanocomposite of polyolefin very important. In this case, as indicated in Figure 1, it was possible to optimize the process for developing a film of exfoliated LDPE nanocompound.

Film Gas Permeability Rates

The average of OPR, CDPR, and WVPR of films is shown in Table IV. Nanoparticles enhanced the barrier effect of films against oxygen, carbon dioxide, and water vapor. As shown in Table III, the OPR, CDPR, and WVPR of the pure PE film were

Table IV. Gas Permeability Rate of the Different LDPE Composites

Sample	O2 transmission (cc-mil m^{-2} day^{-1})	CO2 transmission (cc-mil m^{-2} day^{-1})	Water vapor permeability (g mm kPa^{-1} h^{-1} m^{-2})
PE1	19136.28 ± 260.6^{a}	46084.44 ± 1805^{a}	2.98 ± 0.03^{a}
PE2	11216.79 ± 1365.6^{bc}	32042.8 ± 1167^{c}	2.82 ± 0.07^{a}
PE3	9416.9 ± 749.5^{c}	31204.2 ± 1275^{c}	2.5 ± 0.07^{b}
PE4	17168.2 ± 1545.6^{bc}	43022.9 ± 601.1^{a}	2.89 ± 0.03^{a}
PE5	$12152.76 \pm 1001.3^{abc}$	33635.3 ± 538.1^{bc}	2.93 ± 0.04
PE6	9827.98 ± 1823.8^{bc}	31427.7 ± 673.1^{c}	2.53 ± 0.06^{b}

[a] Each value is the mean of three replicates with the standard deviation. Any two means in the same column followed by the same letter are not significantly ($P > 0.05$) different according to the Duncan's multiple range test.

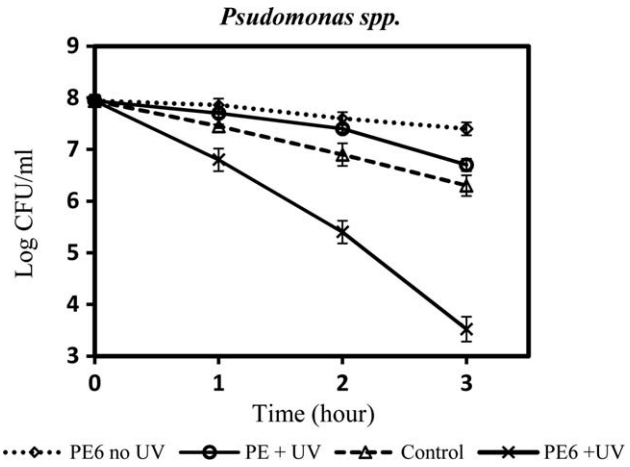

Figure 4. Inactivation of *Pseudomonas* spp. in an *in vitro* test with PE6 and PE1 film under UVA light illumination. Each value corresponds to the mean of three replicates, three plates per replicate. Vertical bar indicates the standard error (SE) [¤: PE6 with no UVA light, Δ: PE1 under UVA light, ○: control (saline solution under UVA light), ×: PE6 film under UVA light].

16202 cc-mil m^{-2} day^{-1}, 39018 cc-mil m^{-2} day^{-1}, and 2.98 g mm kPa^{-1} h^{-1} m^{-2}, as for PE3 film values decreased by 50, 40, and 12%, respectively. The PE6 film showed a slightly higher OPR than the PE3 film. The decrease in gas permeability occurs because the nanoparticles act as a physical obstacle retarding movement gas through the film, slowing down its speed of flow cover to cross the film. Similar results for the reduction of permeability to gases in clay–nanocomposites were reported previously.[23,35] Dispersion of TiO_2 nanoparticles in LDPE matrix slightly modified the barrier properties of PE4 film against oxygen penetration. This behavior can be attributed to a higher orientation of anomaly's tactoids in the clay nanocomposite film and the main transport controlling mechanism could be related to the diffusion through the polymer.[47] The modified barrier properties of nanocomposite films can be increased by the shelf life of food packaging in the film should make the product attractive to deliver markets as the nutritive and organoleptic properties of the food are protected for longer.

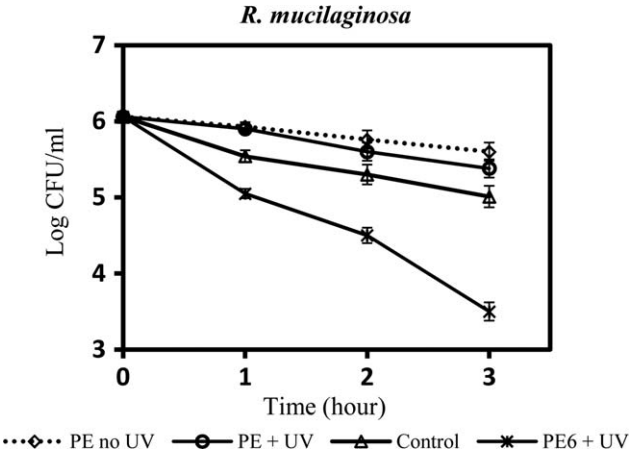

Figure 5. Inactivation of *Rhodotorula mucilaginosa* in an *in vitro* test with PE6 and PE1 film under UVA light illumination. Each value corresponds to the mean of three replicates, three plates per replicate. Vertical bar indicates the standard error (SE) [¤: PE6 film with no UVA light, Δ: PE1 under UVA light, ○: control (saline solution under UVA light), ×: PE6 film under UVA light].

Antimicrobial Activity Evaluation

Antimicrobial evaluation of nanocomposite containing TiO_2 was done on the PE6 film as one of the best samples that possess improved properties in this study. The curves in Figure 4 show that the surviving number of *Pseudomonas* spp. under films without UVA irradiation did not decrease significantly, in accordance with previous results reported for *E. coli*.[23,48–50] This finding demonstrated that nanocomposite film itself did not inactivate microorganisms without UVA light. After exposure to black light illumination, the PE6 film exhibited photocatalytic inactivation. The analyses showed significant differences between the various irradiation times. PE6 film presented lower cell loads (3.49 log CFU mL^{-1}) than PE1 film and control (without sample film under UV) presented higher cell loads (6.3 and 6.7 log CFU mL^{-1}, respectively) after 3 h. The number of surviving *Pseudomonas* spp. decreased by 4.45 and 1.64 log CFU mL^{-1} after 3 h of black light illumination on PE6 film and PE1 film, respectively. The results are very comparable to reductions of 3 and 1 log CFU mL^{-1} found for TiO_2-coated oriented PP (OPP) and uncoated films.[48] This result showed the inactivation of *Pseudomonas* spp. by photoactivation of UVA irradiation. Upon UV light absorption with wavelengths above 250 nm, hydroxyl radicals (•OH) and reactive oxygen species (ROS) generated on the illuminated PE6 nanocomposite film surface play a role in inactivating microorganisms.[51]

The survival rate of *R. mucilaginosa* under all film samples without UVA irradiation did not decrease significantly (Figure 5). At the beginning of the test, the surviving number of yeast was 6.06 log CFU mL^{-1}. The colony count for *R. mucilaginosa* was 3.5, 5.38, and 5.01 log CFU mL^{-1} on the PE6, PE1 films, and control after 3 h of UVA illumination, respectively, corresponding to log CFU reduction of approximately 2.56, 0.68, and 1.05 log CFU mL^{-1}, respectively. Most studies on antimicrobial activity of TiO_2 as a photocatalyst have been done on bacteria, but the first report on the killing mechanism of TiO_2 on yeast (*Saccharomyces cerevisiae*) was reported previously.[52] They presented evidence for the oxidation of coenzyme A (CoA) in *S. cerevisiae* when exposed to light and platinized TiO_2 and found that more than 97% of the intracellular CoA content was lost in the presence of TiO_2 under a metal halide lamp for 120 min, as compared to a 42% loss when TiO_2 was omitted. In this study, the inactivation rate of the two types of microorganisms with LDPE film without nanoparticles and with only UV irradiation decreased compared to that for the PE6 film with no UV exposure, but differences were not statistically significant. These results suggest that the TiO_2 nanoparticles were responsible for the antimicrobial effect when exposed to UVA light illumination. The higher antimicrobial activity of the composite films under UV light is due to the photocatalytic reaction of the TiO_2 nanoparticles in the matrix.

Ethylene Removal Test

Photocatalytic experiments were undertaken to evaluate the effect of TiO_2 nanoparticles in PE6 film for decomposition of ethylene (Figure 6). The columns in Figure 6 show that the

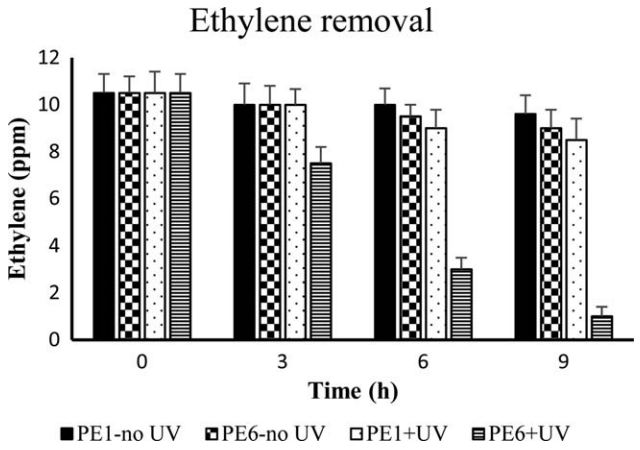

Figure 6. Ethylene removal test by PE1 and PE6 films. Each value corresponds to the mean of three replicates. Vertical bar indicates the standard error (SE) (PE1-no UV: neat LDPE without UVA irradiation, PE6-no UV: clay/TiO_2–LDPE nanocomposite film without UVA irradiation, PE1 + UV: neat LDPE under UVA irradiation, PE6 + UV: clay/TiO_2–LDPE nanocomposite film under UVA irradiation).

ethylene concentration of film sample bags without UVA irradiation did not decrease significantly, in accordance with pervious results reported for TiO_2-coated OPP film.[47] Experimental data show that the TiO_2/clay–nanocomposite loading 3% TiO_2 nanoparticles had photodecomposition efficiency compared to the neat LDPE film (PE1) under UVA irradiation. The concentration of ethylene was reduced to 90% of its initial concentration after 9 h of the UVA irradiation using nanocomposite film, while the concentration of ethylene for the neat LDPE was almost constant. It is clear from Figure 6 that photocatalytic activity of TiO_2 nanocomposite film is strongly influenced by UVA irradiation on sample films. The formation of highly reactive radical species such as hydroxyl radical (•OH) and superoxide anion (O_2^-) under UVA illumination has strong oxidizing power and can oxidize organic and inorganic compounds (photocatalytic degradation).[40] This finding demonstrated that nanocomposite film itself did not decompose ethylene without UV light. After exposure to black light illumination, the PE6 film exhibited photocatalytic degradation. The analyses showed significant differences between the various irradiation times. PE6 nanocomposite film presented higher photodegradation of ethylene (90%) than PE1 film and presented lower photocatalytic degradation (30%) after 9 h.

The higher photodegradation of ethylene by using 10% TiO_2 nanoparticles for coated film was reported in previous studies.[40] In this study, the decomposition of the ethylene was observed using TiO_2 nanoparticles in the TiO_2/clay–LDPE nanocomposite film. This result agreed with[40,53] that the nanoparticles of TiO_2 play a role in the gas-phase photodecomposition efficiency of organic pollutant. It can be considered that the TiO_2 nanoparticles in the plastic film play a significant role in the photocatalytic oxidation of ethylene.[54]

CONCLUSIONS

The nanocomposite thin film of LDPE containing clay and TiO_2 nanoparticles was prepared by the extrusion method. The relative stiffness of nanocomposites increased with the addition of nanoparticles especially clay, with a limited enhancement of the relative yield stress. The XRD spectrum revealed that the distance between the interplanar space (d_{001}), the inactivation, and the nanocompounds increased, confirming the interleaving of the nanoparticles in polymeric matrix; exfoliation of C20A was even achieved in the LDPE studied, as revealed by the elimination of the typical peaks of C20A. The improvement of TiO_2 nanoparticles dispersion in the PE matrix was also checked by XRD. Nanoparticles especially C20A have the capacity to optimize barrier properties. The inactivation of *Pseudomonas* spp. and *R. mucilaginosa* under UVA illumination of the composite films with TiO_2 loading was evaluated. The composite films display excellent antimicrobial activity and ethylene photodegradation. Such nanocomposite film with two kinds of nanoparticles could have promising application as antimicrobial materials with modified barrier properties in fresh horticultural product packaging.

REFERENCES

1. Hong, S. I.; Rhim, J. W. *Food Sci. Technol.* **2012**, *48*, 43.
2. Robertson, G. In Environmentally Compatible Food Packaging; Chiellini, E., Ed.; Woodhead Publishing Ltd: Cambridge, England, **2008**; p 3.
3. Nikkhah, S. J.; Ramazani, S. A. A.; Baniasadi, H.; Tavakolzadeh, F. *Mater. Design* **2009**, *30*, 2309.
4. Yam, K. L. The Wiley Encyclopedia of Packaging Technology; Wiley: New York, **2010**.
5. Chan, C. M.; Wu, J.; Li, J. X.; Cheung, Y. K. *Polymer* **2002**, *43*, 2981.
6. Suwanprateeb, J. *Composites A* **2000**, *31*, 353.
7. Zuiderduin, W.; Westzaan, C.; Huetink, J.; Gaymans, R. *Polymer* **2003**, *44*, 261.
8. Kaleel, S.; Bahuleyan, B. K.; Masihullah, J.; Al-Harthi, M. *J. Nanomater.* **2011**, 2011, 65.
9. Chen, X. D.; Wang, Z.; Liao, Z. F.; Mai, Y. L.; Zhang, M. Q. *Polym. Test.* **2007**, *26*, 202.
10. Nussbaumer, R. J.; Caseri, W. R.; Smith, P.; Tervoort, T. *Macromol. Mater. Eng.* **2003**, *288*, 44.
11. Owpradit, W.; Jongsomjit, B. *Mater. Chem. Phys.* **2008**, *112*, 954.
12. Wang, Z.; Li, G.; Xie, G.; Zhang, Z. *Macromol. Chem. Phys.* **2005**, *206*, 258.
13. Chaichana, E.; Jongsomjit, B.; Praserthdam, P. *Chem. Eng. Sci.* **2007**, *62*, 899.
14. Jongsomjit, B.; Chaichana, E.; Praserthdam, P. *J. Mater. Sci.* **2005**, *40*, 2043.
15. Kontou, E.; Niaounakis, M. *Polymer* **2006**, *47*, 1267.
16. Li, K. T.; Dai, C. L.; Kuo, C. W. *Catal. Commun.* **2007**, *8*, 1209.
17. Golebiewski, J.; Rozanski, A.; Dzwonkowski, J.; Galeski, A. *Eur. Polym. J.* **2008**, *44*, 270.
18. Malucelli, G.; Ronchetti, S.; Lak, N.; Priola, A.; Dintcheva, N. T.; La Mantia, F. P. *Eur. Polym. J.* **2007**, *43*, 328.

19. Morawiec, J.; Pawlak, A.; Slouf, M.; Galeski, A.; Piorkowska, E.; Krasnikowa, N. *Eur. Polym. J.* **2005**, *41*, 1115.
20. Zhao, C.; Qin, H.; Gong, F.; Feng, M.; Zhang, S.; Yang, M. *Polym. Degrad. Stab.* **2005**, *87*, 183.
21. Cioffi, N.; Torsi, L.; Ditaranto, N.; Tantillo, G.; Ghibelli, L.; Sabbatini, L.; Bleve-Zacheo, T.; D'Alessio, M.; Zambonin, P. G.; Traversa, E. *Chem. Mater.* **2005**, *17*, 5255.
22. Shi, Z.; Neoh, K.; Kang, E.; Wang, W. *Biomaterials* **2006**, *27*, 2440.
23. Yu, B.; Leung, K. M.; Guo, Q.; Lau, W. M.; Yang, J. *Nanotechnology* **2011**, *22*, 115603.
24. Fujishima, A.; Rao, T. N.; Tryk, D. A. *J. Photochem. Photobiol.* **2000**, *1*, 1.
25. Fujishima, A.; Hashimoto, K.; Watanabe, T. TiO_2 Photocatalysis: Fundamentals and Applications; BKC Incorporated: Tokyo:, **1999**.
26. Bodaghi, H.; Mostofi, Y.; Oromiehie, A.; Zamani, Z.; Ghanbarzadeh, B.; Costa, C.; Conte, A.; Del Nobile, M. A. *Food Sci. Technol.* **2012**, *50*, 702.
27. Kubacka, A.; Ferrer, M.; Cerrada, M. L.; Serrano, C.; Sanchez-Chaves, M.; Fernández-García, M.; de Andres, A.; Rioboo, R. J. J.; Fernández-Martín, F.; Fernández-García, M. *Appl. Catal. B: Environ.* **2009**, *89*, 441.
28. Maneerat, C.; Hayata, Y. *Int. J. Food Microbiol.* **2006**, *107*, 99.
29. Chavadej, S.; Saktrakool, K.; Rangsunvigit, P.; Lobban, L. L.; Sreethawong, T. *Chem. Eng. J.* **2007**, *132*, 345.
30. Obee, T. N.; Hay, S. O. *Environ. Sci. Technol.* **1997**, *31*, 2034.
31. Zorn, M. E.; Tompkins, D. T.; Zeltner, W. A.; Anderson, M. A. *Environ. Sci. Technol.* **2000**, *34*, 5206.
32. Saltveit, M. E. *Postharvest Biol. Technol.* **1999**, *15*, 279.
33. Kawasumi, M. *Polym. Chem.* **2004**, *42*, 819.
34. Duncan, T. V. *J. Colloid Interface Sci.* **2011**, *363*, 1.
35. Pereira de Abreu, D.; Paseiro Losada, P.; Angulo, I.; Cruz, J. *Eur. Polym. J.* **2007**, *43*, 2229.
36. Zanetti, M.; Camino, G.; Thomann, R.; Mülhaupt, R. *Polymer* **2001**, *42*, 4501.
37. Alamo, R.; Graessley, W.; Krishnamoorti, R.; Lohse, D.; Londono, J.; Mandelkern, L.; Stehling, F.; Wignall, G. *Macromolecules* **1997**, *30*, 561.
38. Ahvenainen, R. *Trends Food Sci. Technol.* **1996**, *7*, 179.
39. Tournas, V.; Heeres, J.; Burgess, L. *Food Microbiol.* **2006**, *23*, 684.
40. Chawengkijwanich, C.; Hayata, Y. *Int. J. Food Microbiol.* **2008**, *123*, 288.
41. Liang, Y.; Wang, Y.; Wu, Y.; Lu, Y.; Zhang, H.; Zhang, L. *Polym. Test.* **2005**, *24*, 12.
42. Thamaphat, K.; Limsuwan, P.; Ngotawornchai, B.; Kasetsart, J. *J. Nat. Sci.* **2008**, *42*, 357.
43. Mina, F. M.; Seema, S.; Matin, R.; Jellur Rahaman, M.; Bijoy Sarker, R.; Abdul Gafur, M.; Abu Hashan Bhuiyan, M. *Polym. Degrad. Stab.* **2009**, *94*, 183.
44. Gopakumar, T.; Lee, J.; Kontopoulou, M.; Parent, J. *Polymer* **2002**, *43*, 5483.
45. Wang, K. H.; Choi, M. H.; Koo, C. M.; Xu, M.; Chung, I. J.; Jang, M. C.; Choi, S. W.; Song, H. H. *J. Polym. Sci. Part B: Polym. Phys.* **2002**, *40*, 1454.
46. Cayer-Barrioz, J.; Ferry, L.; Frihi, D.; Cavalier, K.; Seguela, R.; Vigier, G. *J. Appl Polym. Sci.* **2006**, *100*, 989.
47. Lotti, C.; Isaac, C. S.; Branciforti, M. C.; Alves, R.; Liberman, S.; Bretas, R. E. *Eur. Polym. J.* **2008**, *44*, 1346.
48. Chawengkijwanich, C.; Hayata, Y. In Europe-Asia Symposium on Quality Management in Postharvest Systems-Eurasia, Bangkok, Thailand, Dec 3–6, 2007; Kanlayanarat, S., Hewett, E. W., Ferguson, I. B., Eds.; ISHS Acta Horticulturae 804: Belgium, **2008**.
49. Kikuchi, Y.; Sunada, K.; Iyoda, T.; Hashimoto, K.; Fujishima, A. *J. Photochem. Photobiol. A* **1997**, *106*, 51.
50. Shieh, K. J.; Li, M.; Lee, Y. H.; Sheu, S. D.; Liu, Y. T.; Wang, Y. C. *Nanomed. Nanotechnol. Biol. Med.* **2006**, *2*, 121.
51. Saito, T.; Iwase, T.; Horie, J.; Morioka, T. *J. Photochem. Photobiol. B* **1992**, *14*, 369.
52. Matsunaga, T.; Tomoda, R.; Nakajima, T.; Wake, H. *FEMS Microbiol. Lett.* **1985**, *29*, 211.
53. Maneerat, C.; Hayata, Y. *Trans. ASAE* **2008**, *51*, 163.
54. Park, D. R.; Zhang, J.; Ikeue, K.; Yamashita, H.; Anpo, M. *J. Catal.* **1999**, *185*, 114.